Journal of Chromatography, 327 (1985) 27–45
Elsevier Science Publishers B.V., Amsterdam — Printed in The Netherlands

CHROMSYMP. 585

OPTIMIZATION MODEL FOR THE GRADIENT ELUTION SEPARATION OF PEPTIDE MIXTURES BY REVERSED-PHASE HIGH-PERFORMANCE LIQUID CHROMATOGRAPHY

VERIFICATION OF BAND WIDTH RELATIONSHIPS FOR ACETONITRILE–WATER MOBILE PHASES

M. A. STADALIUS*
Biomedical Products Department, E. I. du Pont de Nemours & Co., Concord Plaza, Wilmington, DE 19898 (U.S.A.)
H. S. GOLD
Department of Chemistry, University of Delaware, Newark, DE 19716 (U.S.A.)
and
L. R. SNYDER
Lloyd R. Snyder, Inc., 2281 William Court, Yorktown Heights, NY 10598 (U.S.A.)

SUMMARY

A previously reported model describes retention and band width as functions of experimental conditions, for the reversed-phase gradient elution separation of peptides and proteins. The model begins by relating separation in gradient elution to corresponding separations by isocratic elution (same high-performance liquid chromatographic system). The use of certain semi-empirical relationships then allows band width to be predicted for samples for which isocratic data are unavailable. This in turn allows the prediction of band width, peak capacity and relative peak height (or peak volume) as a function of experimental conditions such as column dimensions, gradient conditions, mobile phase flow-rate, sample molecular weight, etc. The next paper [*J. Chromatogr.*, 327 (1985) 93] demonstrates the practical value of this approach for optimizing the separation of peptide and protein mixtures.

In the present paper it is first shown that isocratic data for desamido-insulin (6000 daltons) allow the accurate prediction of band widths as a function of experimental conditions in related gradient separations. It is further shown that the present model accurately predicts how band widths vary with experimental conditions for peptides and proteins having molecular weights in the range 600–80 000 daltons.

INTRODUCTION

High-performance liquid chromatography (HPLC) in the reversed-phase gradient elution mode is now widely used for the separation of mixtures of peptides and proteins, especially those with molecular weights of less than 30 000 daltons (*e.g.*,

0021-9673/85/$03.30

refs. 1–4). In the separation of low-molecular-weight samples (< 1000 daltons) by reversed-phase HPLC, the choice of column configuration and stationary phase composition can significantly affect band widths and separation. A considerable body of work has been reported on similar effects in analogous separations of peptides and proteins (*e.g.*, refs. 2–20 and especially refs. 4 and 20). However many of the reported conclusions are contradictory, and an optimum choice of column for a particular separation is at present by no means clear. For example, some workers have reported improved band shape, narrower bands and/or better recovery from column packings having shorter alkyl chains[8,9,13,18,19], while other workers have reported no differences[3,6,7,10], at least for alkyl groups from C_3 to C_8. Likewise some workers have reported that maximally-bonded and end-capped alkyl-silica packings are optimum as regards band width, band shape and recovery[1,3,5,10], while other workers find little effect of end capping on separation[7]. Finally there is a continuing controversy over whether the plate number N of a column as measured for small molecules is related to the column N value for large-molecule separations (*e.g.*, refs. 16, 18 and 21), or even whether column plate number has any relevance to large-molecule separations (*e.g.*, refs. 21 and 22).

There are many reasons why previous work on band width and related separation phenomena should appear puzzling as regards these separations of peptides and proteins. Early workers noted that plate numbers (N) for peptide/protein separations were often quite small when compared with N values for the corresponding separation of small molecules (*e.g.*, refs. 11 and 12). This effect is now believed due to the smaller diffusion coefficients of proteins, which increase the reduced velocity of the mobile phase (other conditions comparable) (*e.g.*, ref. 23). This effect of slow diffusion of large molecules in the mobile phase is further enhanced when the column-packing pore-diameter approaches the Stokes diameter of the diffusing protein molecule (*e.g.*, refs. 20, 24 and 25), leading to still lower values of N. Likewise many workers have noted that change in column dimensions, flow-rate or other conditions seems to affect the gradient separation of peptide/protein samples differently than for isocratic separations of small molecules (*e.g.*, refs. 21 and 22). However these effects are expected and predictable from the present theory of gradient elution[23,26].

As opposed to the foregoing *apparent* reasons for band-width differences between peptide/protein separations and separations of small molecules, there are a number of *real* complications in the HPLC separation of proteins. Secondary retention processes (*e.g.*, binding of solute to silanol groups on the column packing) can contribute significantly to band broadening (*e.g.*, refs. 3 and 20). This is apparent in the separation of basic peptides and proteins, where addition of amine modifiers to the mobile phase can drastically reduce both band tailing and band width[7,27]. Proteins also exist in different conformations (native *vs.* denatured), and the slow equilibrium between different forms can dramatically increase band width and worsen band shape[20,28–30] as well as possibly explain other anomalies observed in these protein separations (*e.g.*, variation of isocratic k' values with mobile phase flow-rate[31]). We will refer to separation systems exhibiting these latter effects as not "well behaved".

We have previously reported a model[31] that describes the separation of peptide/protein samples by reversed-phase gradient elution. While this model is based on the general theory of small-molecule separations (*e.g.*, ref. 32), it takes into ac-

count any differences of large-molecule separations for "well-behaved" systems; *i.e.* those free of secondary retention and slow equilibration effects as discussed above[7,20,27–30]. The model has been shown to accurately describe solute retention. Thus given isocratic retention data for a solute as a function of experimental conditions (column, mobile phase composition and flow-rate, temperature, etc.), it is possible to predict retention in "corresponding"* gradient systems as a function of gradient conditions (gradient time t_G, gradient range $\Delta\varphi$, flow-rate F, etc.). In the absence of isocratic retention data, a few gradient runs can be used to derive isocratic parameters, which can then be used to predict gradient retention as a function of change in experimental conditions (t_G, $\Delta\varphi$, F, etc.).

In this paper the experimental verification of the model is extended by the prediction of gradient band widths, either on the basis of isocratic measurements in corresponding HPLC systems, or simply as a function of experimental gradient conditions. We have thus established that the present model can accurately predict band widths as a function of experimental conditions for the separation of peptide/protein samples by reversed-phase gradient elution. In the following paper[33] and elsewhere[34] we show some practical applications of this model, and we further explore its implications for understanding band widths as a function of column design.

THEORY

The initial model and its theory have been described in ref. 31. In this study we have modified parts of this model on the basis of new experimental data and further theoretical analysis. We have also simplified some previously derived relationships and made them more general. For these reasons we will review the essential elements of the model here. The starting points for the model are the general theory of chromatographic band widths or plate numbers N, as detailed in ref. 32, and the theory of linear-solvent-strength (LSS) gradient elution as given in refs. 26, 31, 35 and 36. The following set of equations forms the basis of the computer program described in the following paper[33]. Since these equations for the most part have been derived and justified in the preceding paper[31], they are simply arranged in the order required for calculation of final values of band width. For further details see ref. 31.

The linear velocity of the mobile phase within the column (u) is given by

$$u = LF/V_m \tag{1}$$

where L is column length (cm), F is flow-rate (ml/sec), and V_m is the column dead volume (ml). V_m is given as

$$V_m = (\pi/10)d_c^2\, L/x \tag{2}$$

where d_c is the column internal diameter (cm) and x is the fraction of mobile phase

* By "corresponding" gradient and isocratic systems, we mean the use of the same column and temperature, with the mobile phase in each case formed from two solvents A and B which are the same (*e.g.*, mixtures of water and methanol). Retention of a given solute under isocratic or gradient conditions is then related theoretically, as described in ref. 26.

within the column that is outside the pores of the particles. The reduced velocity v can be defined:

$$v = ud_p/D_m \tag{3}$$

The quantity d_p is the particle diameter of the column packing (cm), and D_m is the diffusion coefficient of the solute in the mobile phase (cm/sec). The diffusion coefficient can be expressed as a function of temperature and solute molecular weight by the semi-empirical relationship[31]

$$D_m = (9 \cdot 10^{-6})\,(T/298)^7\,(2.2\,M^{-1/3} + 62\,M^{-1})/\eta_{25} \tag{4}$$

Here T is temperature (°K), M is the sample molecular weight (daltons), and η_{25} is the average mobile phase viscosity at 25°C (see ref. 31). Eqn. 4 is in agreement with other semi-empirical equations for protein diffusion coefficients as a function of molecular weight (at ambient temperature, see refs. 37 and 38), and with the Wilke-Chang equation[39] when $M < 1000$. The reduced plate height h (equal to H/d_p), is given by the Knox equation (see ref. 32):

$$h = Av^{1/3} + B/v + Cv \tag{5}$$

The quantity v is the reduced velocity (equal to $u\,d_p/D_m$) and A, B and C are defined as follows. A is an empirical constant that measures how well the column has been packed; typical values of A range from 0.5 to 1.0 and are constant for a given column, regardless of other experimental conditions. The quantity B is a measure of how fast solute molecules diffuse within the column; B includes contributions from molecules in both the mobile and stationary phases:

$$\begin{aligned} B &= a' + b'k' \\ &\approx 1.1 + b'k' \end{aligned} \tag{6}$$

The parameter b' equals the ratio of solute diffusion coefficients in the stationary and mobile phases, respectively, and is a function of both solute molecular weight and the pore-diameter of the pores of the column-packing. Values of b' were determined in the present study by fitting experimental band width data to the present model; values of b' can range from 0 to 1. The quantity $\bar{k}$ is the mean or effective capacity factor k' during gradient elution[26]. The parameter C is a measure of how fast solute molecules diffuse through the pores of the column packing:

$$C = [(1 - x + \bar{k})/(1 + \bar{k})]^2/15\,\rho\,(B - 1.28x) \tag{7}$$

The quantity ρ represents a decrease in D_m as a result of restricted diffusion of large molecules within small pores. Like b', ρ is a function of solute molecular weight and the pore-diameter of the column-packing pores, and also varies from 0 to 1. Values of ρ in the present study were determined by fitting experimental band width data to the present model. The effective capacity factor $\bar{k}$ for gradient elution is the value of k' for the band when it reaches the column midpoint; $\bar{k}$ is related to experimental gradient conditions as

$$\bar{k} = F\,t_G/(0.5 \ln 10)\,\Delta\varphi\,S\,V_m \tag{8}$$

Here t_G is the gradient time (time from beginning to end of the gradient), $\Delta\varphi$ is the change in volume-fraction φ of the organic solvent in the mobile phase during the gradient, and S equals $-\mathrm{d}(\log k')/\mathrm{d}\varphi$. Values of S have been empirically related to solute molecular weight as

$$S = 0.48\ M^{0.44} \tag{9}$$

for the case of peptide and protein solutes, and acetonitrile as organic solvent. Stronger organic solvents such as isopropanol have larger values of S[31], and strongly denaturing solvents such as formic acid yield values of S that are roughly proportional to values of M[40]. The column plate number N is now calculable as

$$N = L/H = L/h\ d_p \tag{10}$$

The theoretical value of the band width (1 S.D.) expressed in volume units (ml) is

$$\sigma'_v = t_G\ F(1 + \bar{k})/(\ln 10)\ S\ \Delta\varphi\ N^{1/2}\bar{k} \tag{11}$$

However it has been found[26,41] and confirmed in this study that experimental values of σ_v are larger than values predicted by eqn. 11, by an empirical factor J:

$$\sigma_v = J\ t_G\ F(1 + \bar{k})/(\ln 10)\ S\ \Delta\varphi\ N^{1/2}\bar{k} \tag{11a}$$

The factor J will be shown here to be a function of $\bar{k}$; J is approximately independent of other experimental conditions when acetonitrile is used as organic solvent. Experimental values of J can be described by the following polynomial:

$$J = 0.99 + 1.70\ b - 1.35\ b^2 + 0.48\ b^3 - 0.062\ b^4 \tag{12}$$

where

$$b = 1/0.5(\ln 10)\ \bar{k} \tag{13}$$

The basic phenomenon which leads to values of $J > 1$ is not yet understood. Work in our laboratory is continuing in an effort to better define this effect. Unreported studies suggest that the "J-effect" is also found in the gradient separation of proteins by ion exchange, and its magnitude appears to be given approximately by eqn. 12. The band width σ_v can also be expressed in time units (sec):

$$\sigma_t = \sigma_v/F \tag{14}$$

Band width can be corrected for extra-column band-broadening as discussed in ref. 42, eqns. 5–5b). This leads to the following corrected value of σ_v:

$$\sigma_{v(corr)} = [\sigma_v^2 + \sigma_{ec}^2 + (F\tau)^2]^{1/2} \tag{15}$$

Here σ_{ec} is the extra-column contribution to σ_v due to the volume of the HPLC system; a typical value of σ_{ec} for "recent" HPLC systems is about 0.02 ml. The

quantity τ is the detector time constant, which varies from 0.1 to 1 sec for most photometric detectors. Band width can also be expressed in terms of the peak capacity of the chromatogram (PC):

$$PC = F\, t_G/4\, \sigma_v \tag{16}$$

Average resolution R_s is proportional to PC.

Eqns. 11a, 15, 16 allow the calculation of peak capacity and average band width as a function of sample molecular weight and experimental gradient conditions, when certain column parameters (b', ρ) are known. Alternatively, experimental values of σ_v or PC can be fit to the model, using "best fit" values of b' and ρ.

EXPERIMENTAL

Apparatus

The liquid chromatographic detection used in this study was performed with a Du Pont Series 8800 with UV spectrophotometer (Du Pont, Wilmington, DE, U.S.A.). Chromatographic data for all isocratic and gradient data were obtained in real time using the Du Pont PDP-10 Dart Analysis System.

Reagents

HPLC grade acetonitrile (J. T. Baker, Phillipsburg, NJ, U.S.A.) and purified water from a Milli-Q system are the mobile phase solvents. Reagent grade trifluoroacetic acid (TFA) (Eastman Kodak, Rochester, NY, U.S.A.) was purified weekly by distillation over chromium trioxide. Gold-label morpholine (Aldrich, Milwaukee, WI, U.S.A.) and HPLC-grade phosphoric acid (Fisher Scientific, Fair Lawn, NJ, U.S.A.) were used as obtained. The peptides and proteins (leucine enkephalin, bradykinin, angiotensin, glucagon, insulin, ribonuclease A and lysozyme) were obtained from Sigma (St. Louis, MO, U.S.A.).

Over time insulin is irreversibly converted into its desamido form. This is catalyzed by an acidic environment. Since the desamido form interfered with the peak-width determination at very low k' and $\bar{k}$ values, the desamido form was isolated preparatively, as described in ref. 31.

Column

The experimental packing used in this study is a 4.8-μm, 15-nm pore, silica-based particle bonded with octyldimethylchlorosilane (C_8) and capped with trimethylchlorosilane. The 8.0 × 0.62 cm I.D. column configuration was packed using standard slurry-packing procedures. Similar columns are available from Du Pont as Bioseries® PEP-RPI.

Procedure

The stability of the column was checked frequently by evaluating k', skew and efficiency for a diamyl phthalate peak eluted with a mobile phase of acetonitrile (unmodified)–water (66:34) at 35°C. The column efficiency was constant at approximately 6000 plates, with a skew value[39] that did not exceed 0.20 ($k' = 5.0$).

Isocratic efficiency data for desamido-insulin were obtained using the software

program CRAPS, available on the PDP-10 Dart real-time analysis system (Du Pont Experimental Station, Wilmington, DE, U.S.A.). This program reports first- and second-moment plate numbers. Agreement between first- and second-moment plate numbers was generally good (±10%). First-moment plate numbers are reported here.

The peptide and protein gradient-bandwidths were obtained using the software program COLPR. Each gradient run was stored on disk, so that off-line data reduction, using the GC.MON program, was possible. GC.MON, when operated from a graphics terminal, offers scale expansion and cursor options which were used to accurately measure the bandwidth of each peak in every gradient run. This procedure provided an internal check for those values reported by COLPR. COLPR had difficulty calculating bandwidth values for peaks eluted with very steep gradients: it consistently reported high values of σ. These questionable bandwidth values were then replaced with those measured using the graphics software options.

The extra-column volume of this system which contributes to band broadening is 20 μl (σ_{ec}). This was determined by first replacing the column with 8 cm of 0.01-in.-diameter stainless-steel tubing and allowing an acetonitrile–water (80:20) mobile phase to flow at 0.30 ml/min through the system. Then, 2 μl of a dilute solution of diamyl phthalate in acetonitrile–water (4:1) was injected into the system and the resulting peak was recorded using a relatively fast chart speed (3 in./min). The measured bandwidth of this peak (in volume units) corresponds to the extracolumn volume of the system. Another study has shown[41] that σ_{ec} is weakly dependent on flow-rate, but it is assumed here that σ_{ec} is constant, to a first approximation. The time constant (τ) of the system, (supplied by Du Pont Instrument Engineering Department), was reported to be 1 sec. This was verified by eluting 2 μl of the same diamyl-phthalate solution from the system at 5.00 ml/min and calculating the bandwidth of the resulting peak in time units. The time constant of the detector using this method was calculated to be 0.9 sec.

RESULTS AND DISCUSSION

Our approach to developing and confirming the present model (for separations of peptides and proteins by gradient elution) has proceeded in stages. First we have confirmed and further developed the theory of band broadening for small molecules in isocratic separation[32]. Second we have shown that retention for small molecules in gradient elution can be predicted accurately from corresponding retention data in isocratic separation[26,35], and *vice versa*[36]. Third we have reported that retention for large molecules in gradient elution can be predicted from corresponding data for isocratic separation: polystyrenes[36,43] and peptides/proteins[31]. In this paper it remains to confirm the theory of band broadening in the gradient separation of small molecules, and to extend this treatment to the similar separations of large molecules (peptides and proteins).

Band broadening of small molecules in gradient elution

For linear-solvent-strength gradient elution, only limited data have been reported which attempt to predict band widths as a function of experimental conditions[26,41,44,45]. For acetonitrile–water mobile phases (as in the present study) and small molecule solutes, these previous data suggest that eqn. 11 is reasonably accurate

when $\bar{k}$ is large. However, when $\bar{k}$ is small it appears that experimental band widths (σ_v) are larger than values predicted by eqn. 11; the reason for this experimental discrepancy is at present not known. This anomalous behavior is illustrated in Fig. 1a, using data (●, ■) that were reported previously. These latter data-points in Fig. 1a required calculated values of σ_v, predictable (as a function of k') from our earlier study[32] and further detailed in ref. 46. It is seen in Fig. 1a that the ratio of experimental σ_v values to calculated values $[\sigma_{v(expt)}/\sigma_{v(calc)}] = J$ is close to unity at small values of the gradient parameter b (large values of $\bar{k}$), but increases with b and approaches a limiting value of about 1.8. That is, for steep gradients and small values of $\bar{k}$, experimental band widths can be almost double the predicted values.

To confirm this anomalous band broadening in gradient elution for small molecules and the presently studied HPLC system (same column, acetonitrile–water mobile phase), we carried out additional measurements as summarized in Tables I and II. Two small-molecule solutes, di-*n*-pentyl (C_5) and di-*n*-octyl (C_8) phthalate, were run under corresponding isocratic and gradient conditions (same column, same mobile phases, etc.), and band widths for both cases were compared. The isocratic data of Table I were first correlated with the band width model of ref. 32, based on eqns. 1–7, and 10 (k' replaces $\bar{k}$). The column parameter b' was assumed equal to 0.40, on the basis of data in ref. 32, and experimental values of N (Table I) were best-fit to a value of the column parameter ρ ($\rho = 0.55$). Resulting values of N (cal-

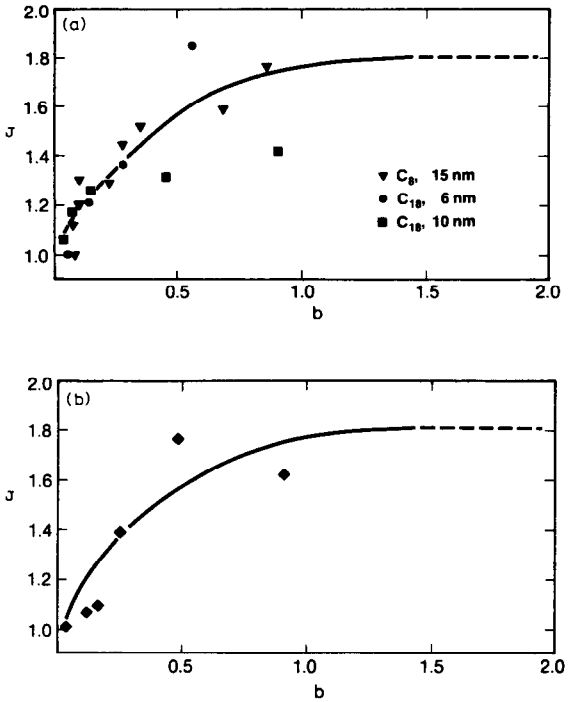

Fig. 1. Plot of J-factor (equal to $\sigma_{expt}/\sigma_{calc}$) *vs.* gradient steepness parameter b for acetonitrile–water mobile phases. (a) ●, from ref. 43; ■, from ref. 44; ▼, phthalates of Table II. (b) Data for desamido-insulin from Table IV. ----, calculated value of J from eqn. 12.

TABLE I

PLATE NUMBERS FOR ISOCRATIC ELUTION OF C_5 AND C_8 PHTHALATES AS A FUNCTION OF k' AND FLOW-RATE

Acetonitrile–water mobile phase at 35°C; 8 × 0.62 cm I.D. column packed with 15-nm pore, C_8 bonded silica; column parameters used: $x = 0.67$, $A = 0.6$, $d_p = 4.8$ μm, $a' = 1.1$, $A = 0.60$, $b' = 0.40$ and $\rho = 0.55$. Values in parentheses are calculated values.

Solute	φ	k'	N_{expt} (N_{calc})	
			1.00 ml/min	*4.00 ml/min*
C_5	0.72	1.4	6220 (6140)	–
C_5	0.78	2.0	6620 (6932)	–
C_5	0.82	3.1	6720 (7590)	–
C_8	0.72	5.5	7740 (7680)	5600 (4720)
C_8	0.78	9.3	6780 (6780)	–
C_8	0.82	16.0	5970 (5690)	6270 (6408)

culated) in Table I agree reasonably well with experimental values: ±9% (1 S.D.), equivalent to ±5% in calculated values of σ_v.

The experimental values of σ_v in Table II for gradient elution were likewise compared with values calculated from eqns. 1–11, using the derived value of ρ from the data of Table I (other column parameters also as in Table I). The last column of Table II compares experimental and calculated values of σ_v for these small-molecule gradient separations. It is seen that the ratio $[\sigma_{v(expt)}/\sigma_{v(calc)}] = J$ is close to unity for small values of b, but increases regularly as b increases beyond 0.1. These ratios are plotted *vs.* b in Fig. 1a (▼), along with data from the previous literature. Most of these data points fall reasonably close to the solid curve of Fig. 1a (eqn. 12). The error in J (eqn. 12 *vs.* $\sigma_{expt}/\sigma_{calc}$ from Table II) is only ±5% (1 S.D.), which is equal to the error in calculated values of N in Table I (±5% in σ_v, 1 S.D.). All data of Fig.

TABLE II

SUMMARY OF CALCULATED AND EXPERIMENTAL GRADIENT BANDWIDTH DATA FOR C_5 AND C_8 PHTHALATES AS A FUNCTION OF GRADIENT STEEPNESS, b

Same mobile phase, column and column parameters as Table I.

Solute	*Flow-rate (ml/min)*	$\Delta\varphi$	t_G	σ_{expt}	b	$\sigma_{expt}/\sigma_{calc}$*
C_5	1.00	0.60	40	108	0.08	1.00
C_8	2.00	0.60	20	117	0.08	1.12
C_5	1.00	0.60	40	103	0.10	1.22
C_8	2.00	0.60	20	112	0.10	1.30
C_5	1.00	1.00	20	60	0.27	1.43
C_8	1.00	1.00	20	56	0.35	1.47
C_5	1.00	1.00	8	49	0.68	1.59
C_8	1.00	1.00	8	53	0.86	1.75

* σ_{calc} from eqn. 11a.

1 fall reasonably close to a single curve of J *vs.* b, for these three studies from different laboratories; this suggests that eqn. 12 should be reliable for estimating the "anomalous band broadening effect" in gradient elution. However all the data of Fig. 1 are for acetonitrile–water as mobile phase, and there are some indications that other organic solvents may not show this effect to the same degree (see Fig. 40 of ref. 26) and related discussion).

Band broadening of peptides and proteins in gradient elution

Results for desamido-insulin. Band width for desamido-insulin in isocratic separation was next studied as a function of k' and flow-rate. The experimental data are summarized in Table III. Again the data were best-fit to the column parameters b' and ρ: $b' = 0.15$ and $\rho = 0.45$. The resulting agreement of experimental and isocratic data was poorer than observed for the phthalates of Table I: ±16% in calculated values of σ_v (Table III), *vs.* ±5% for the data of Table I. This may be due to the "peculiarities" of biochemical systems and the fact that desamido-insulin is not perfectly "well behaved"[31].

Data for the separation of desamido-insulin in a corresponding gradient system were obtained next, as summarized in Table IV. Using the column parameters of Table III for isocratic separation, gradient band widths could be predicted for the separations of Table IV (eqn. 11a). Also, the ratio J could be obtained as before ($\sigma_{expt}/\sigma_{calc}$), and these values (from Table IV) are plotted in Fig. 1b, with the J-function from Fig. 1a (eqn. 12) superimposed. It is seen that eqn. 12 provides a close fit to these experimental values of J *vs.* b. Thus eqn. 12 appears to be reasonably general for the gradient separation of both small and large molecules, at least for reversed-phase systems and acetonitrile–water as mobile phase. We will assume the validity of eqn. 12 in further discussion here, and all calculated values of σ_v will be based on eqn. 11a (which takes the J-effect into account).

The final agreement of experimental and calculated band widths for desamido-insulin (data of Table IV, including correction for J), is ±14% (1 S.D.). Con-

TABLE III

PLATE NUMBERS FOR ISOCRATIC ELUTION OF DESAMIDO-INSULIN AS A FUNCTION OF MOBILE PHASE COMPOSITION φ AND FLOW-RATE

Acetonitrile–water mixtures with 0.1% (v/v) morpholine and 0.125% (v/v) TFA added (pH = 2.2); 8 × 0.62 cm I.D. column packed with 15-nm pore, C_8-bonded silica, temperature 35°C. Column parameters: $x = 0.67$, $a' = 1.1$, $d_p = 4.8$, $b' = 0.15$, $\rho = 0.45$.

φ	k'	N_{exp} (N_{calc})				
		Flow-rate (ml/min)				
		0.50	*1.0*	*2.0*	*4.0*	*6.0*
0.29	20.5			2500 (3490)	1420 (2130)	1150 (1550)
0.30	9.1		3350 (3940)	2320 (2370)	1610 (1340)	1250 (930)
0.31	7.0	4840 (4500)	3140 (3560)	2050 (2190)		
0.32	3.5		3240 (2740)	2200 (1540)	1370 (1150)	1040 (530)
0.34	1.6		2260 (2140)	1830 (1160)		

TABLE IV

SUMMARY OF GRADIENT BANDWIDTH DATA FOR DESAMIDO-INSULIN AS A FUNCTION OF GRADIENT STEEPNESS, b

Same mobile phase and column as Table III. Column parameters used are identical to parameters of Table III. See text for further details.

φ	t_G(min)	Flow-rate (ml/min)	b	J-factor*	σ_{expt}	σ_{calc}**
0.40	10	1.0	1.27	1.44	52	52
0.35	12	1.0	0.92	1.61	63	57
0.30	20	1.0	0.48	1.76	86	69
0.28	35	1.0	0.25	1.38	91	85
0.30	28	2.0	0.17	1.08	119	133
0.30	40	2.0	0.12	1.07	144	156
0.30	20	4.0	0.12	1.01	187	212
0.25	60	3.0	0.04	–	370	315

* σ_{calc} from eqn. 11.
** Eqn. 11a.

sidering the fit of isocratic band widths (±16%, Table III), this agreement appears reasonable.

Results for other peptides and proteins. Band width data were obtained by us for six other peptides and proteins, using gradient elution with a broad range of experimental conditions (values of gradient time, flow-rate and gradient range). These data are summarized in Table V. For each solute the band width data were best-fit to values of the column parameters b' and ρ, as summarized in Table V. Resulting calculated values of σ_v were in good agreement with experimental σ_v values; for all data of Table V the agreement was ±13% (1 S.D.). To show this more clearly, experimental values of σ_v for these compounds are plotted *vs.* calculated values in Fig. 2.

The σ_v values of Tables IV and V are seen to vary widely with experimental conditions (values of t_G, F and φ). The origin of this variability of σ_v values can be seen in eqn. 11a, but is perhaps more clear by combining eqns. 8 and 11a to give

$$\sigma_v = 0.5\, J\,(1 + \bar{k})\, V_m\, N^{-1/2} \tag{18}$$

With column dimensions (and V_m) held constant in these studies, and since J is a function of $\bar{k}$ (eqns. 12 and 13), it is seen that band width depends on average capacity factor $\bar{k}$ and on the plate number of the column. This is closely analogous to the case of band widths in isocratic separation, which are given as

$$\sigma_v = (1 + k')\, V_m\, N^{-1/2} \tag{19}$$

Results for lysozyme digest. While our model shows good agreement with experimental band widths for the peptides and proteins in Tables III–V, it might be argued that "real" peptide sample are subject to other effects and could therefore show poorer agreement. This should be especially true of tryptic digests, since every peptide will have a terminal basic amino acid — and such peptides have been shown to be more prone to band tailing and to give wider bands[7]. We therefore ran several

TABLE V

SUMMARY OF GRADIENT BANDWIDTH DATA FOR PEPTIDES AND PROTEINS OF VARYING MOLECULAR WEIGHT AS A FUNCTION OF GRADIENT CONDITIONS

Same mobile phase and column as in Table III. Column parameters: $x = 0.67$, $A = 0.60$, $d_p = 4.8$.

Solute	$\Delta\varphi$	t_G *(min)*	*Flow-rate (ml/min)*	σ_{expt}	σ_{calc}	*Solute*	σ_{expt}	σ_{calc}
Leucine enkephalin	0.40	10	1.00	44	44	Angiotensin I	49	48
600 daltons	0.35	12	1.00	48	48	1300 daltons	53	52
$S = 11$	0.30	20	1.00	68	59	$S = 15$	83	63
$b' = 0.20$	0.28	35	1.00	92	81	$b' = 0.15$	92	80
$\rho = 0.55$	0.30	28	2.00	130	122	$\rho = 0.45$	132	125
S.D. of fit 17%	0.30	40	2.00	141	155	S.D. of fit 11%	149	151
	0.30	20	4.00	181	192		206	198
	0.25	60	3.00	272	376		328	332
Bradykinin	0.40	10	1.00	56	52	Glucagon	44	48
1100 daltons	0.35	12	1.00	–	–	3500 daltons	–	–
$S = 13$	0.30	20	1.00	89	75	$S = 22$	61	64
$b' = 0.05$	0.28	35	1.00	132	102	$b' = 0.15$	83	79
$\rho = 0.45$	0.30	28	2.00	176	167	$\rho = 0.45$	112	123
S.D. of fit 13%	0.30	40	2.00	229	205	S.D. of fit 9%	164	144
	0.30	20	4.00	260	276		190	196
	0.25	60	3.00	418	450		321	293
Ribo-nuclease A	0.40	10	1.00	51	55	Lysozyme	62	67
12 500 daltons	0.35	12	1.00	–	–	14 000 daltons	93	74
$S = 40$	0.30	20	1.00	75	76	$S = 40$	–	–
$b' = 0.10$	0.28	35	1.00	96	95	$b' = 0.05$	130	129
$\rho = 0.30$	0.30	28	2.00	150	153	$\rho = 0.20$	187	216
S.D. of fit 10%	0.30	40	2.00	217	176	S.D. of fit 14%	235	256
	0.30	20	4.00	226	247		315	362
	0.25	60	3.00	370	332		480	518

gradient separations of a lysozyme tryptic digest, as summarized in Table VI. A typical chromatogram for this separation is shown in Fig. 3. For a limited range in conditions, the average band widths measured in these runs (using well resolved, major peaks) are seen to agree closely with values calculated from the model (± 11% in σ_v, 1 S.D.). Additional data on this same sample are provided in the following paper[33], again with good agreement between experimental and calculated values.

Other band broadening studies from the literature

We have examined two other studies from the literature which present bandwidth data in the reversed-phase gradient separation of peptide/protein samples. In each case results were presented for the same sample and a wide range of gradient conditions (gradient time and flow-rate varied). We were also able to obtain addi-

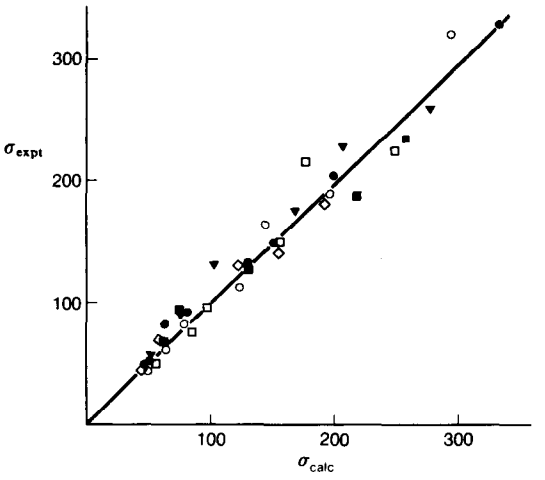

Fig. 2. Comparison of experimental *vs.* calculated values of σ_v for peptides of Table V. Calculated values from eqn. 11a. ●, Angiotensin; ○, glucagon; □, ribonuclease A; ▼, bradykinin; ■, lysozyme; ◇, leucine enkephalin.

tional information from the authors of these two studies, which facilitated comparisons of their data with our model.

We have commented earlier[31] on the study of Meek and Rosetti[12], who separated a peptide mixture (average molecular weight of 1100) on an 8-nm-pore C_{18} column. Our correlation in ref. 31 neglected to consider the *J*-ratio, and we have since recalculated these data. Our final correlation shows best-fit values of $b' = 0.20$ and $\rho = 0.35$, with an agreement of $\pm 13\%$ (1 S.D.) in calculated values of σ_v.

A second literature study that can be correlated with out model is that of Nice *et al.*[13], who separated a seven-protein sample on a 30-nm-pore C_4 column (gradient elution with gradient time and flow-rate varied over wide limits). Their data (kindly supplied to us by Dr. Nelson Cooke) are summarized in Table VII, along with cal-

TABLE VI

AVERAGE BAND WIDTH DATA FOR TRYPTIC DIGEST OF LYSOZYME. COMPARISON OF EXPERIMENTAL *vs.* CALCULATED VALUES FOR VARYING GRADIENT TIMES AND FLOW-RATES

Same mobile phase and column as in Table III. $\Delta\varphi = 0.32$, $d_p = 4.8$ μm, $T = 35$°C. Column parameters: $x = 0.67$, $b' = 0.20$, $\rho = 0.50$.

t_G (min)	F (ml/min)	σ_v	
		expt.	*calc.**
45	0.5	54	55
45	1.0	91	91
45	2.5	194	215
15	0.5	46	39
15	1.0	54	57
15	2.5	100	114

* Eqn. 11a.

TABLE VII

SUMMARY OF PEAK CAPACITY DATA FOR PROTEINS[13] SEPARATED ON 30-nm PORE, C_4-BONDED SILICA (7.5 × 0.46 cm)

Acetonitrile–water containing 0.01 *M* TFA mobile phase at room temperature, $\Delta\varphi$ maintained constant at 0.48. Column parameters: $x = 0.7$, $d_p = 10$ μm, $A = 0.60$.

Ribonuclease A, lysozyme and cytochrome c (Average MW = 12 800, b′ = 0.20; ρ = 0.90; S.D. of fit ± 19%)				*Carbonic anhydrase (30 000 daltons; b′ = 0.1; ρ = 0.40; S.D. of fit ± 17%)*				*Transferrin (80 000 daltons, b′ = 0.0; ρ 0.3; S.D. of fit ± 16%)*			
Flow-rate (ml/min)	t_G	PC_{expt}	PC_{calc}	*Flow-rate (ml/min)*	t_G	PC_{expt}	PC_{calc}	*Flow-rate (ml/min)*	t_G	PC_{expt}	PC_{calc}
0.25	384	225	285	0.25	384	–	–	0.25	384	114	119
	192	201	204		192	125	132		192	88	95
	96	134	134		96	82	86		96	55	70
	48	102	84		48	66	57		48	52	51
0.50	192	–	–	0.50	192	–	–	0.50	192	77	86
	96	137	159		96	87	96		96	54	67
	48	120	102		48	64	62		48	46	50
	24	83	64		24	44	42		24	37	37
1.00	96	145	176	1.00	96	89	104	1.00	96	65	60
	48	121	120		48	64	69		48	48	47
	24	91	76		24	50	45		24	46	36
	12	57	48		12	38	30		12	30	26
2.00	48	102	133	2.00	48	78	78	2.00	48	46	43
	24	77	89		24	35	49		24	26	33
	12	64	56		12	–	–		12	–	–
	6	49	35		6	28	21		6	24	19

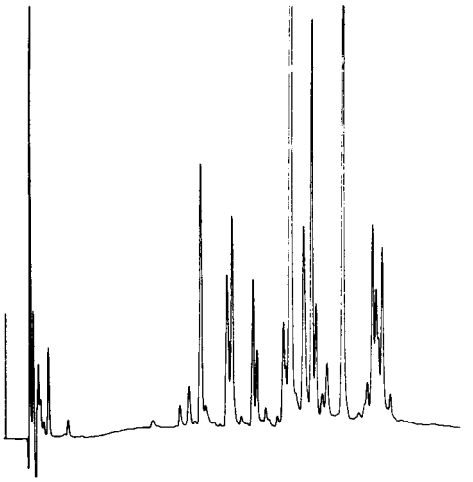

Fig. 3. Chromatogram of lysozyme digest separated on Bioseries® PEP-RP1 column. Linear gradient from 8 to 40% acetonitrile–water (TFA and morpholine added), gradient time = 15 min, flow-rate = 1.5 ml/min.

culated values of σ_v. We have excluded bovine serum albumin and ovalbumin from the study of ref. 13, as these compounds exhibit poor peak shape and are apparently not "well behaved" in the system of ref. 13. For convenience we also averaged the band widths for the three smaller proteins of similar M value: ribonuclease A, lysozyme and cytochrome c. The resulting calculated values of PC in Table VII (best-fit to b' and ρ for each solute) agree with experimental values, within $\pm 18\%$ (1 S.D.) overall.

Correlation of column parameters b' and ρ with solute molecular weight and column-packing pore diameter

The preceding examples show that our model does a reasonable job of correlating experimental band-width data for the reversed-phase gradient separation of mixtures of peptides and proteins. A further test of the model is afforded by the derived column parameters b' and ρ. According to theory[20,24,25,33] both b' and ρ should decrease as sample molecular weight increases and/or column-packing pore-diameter decreases. This was found to be the case generally, as summarized in the data of Table VIII. While there is some scatter in these data, there is a general trend to lower values of b' and ρ as M increases and pore-diameter decreases. It should be noted that the fit of experimental and calculated σ_v values is not very sensitive to change in b' and ρ; the values of Table VIII may not be any more accurate than ± 0.1 units in b' or ρ. We are further analyzing the dependence of these column parameters on M and pore-size, and will report on this at a later time.

An overview of the present model

The many phenomena that enter into the present model suggest that the overall process of gradient elution as applied to large biomolecules is fairly complex. Additionally, secondary effects such as have been cited[7,20,27–30] can further complicate actual separations. In view of the various empirical parameters (A, b', ρ, J and a'

TABLE VIII

CORRELATION OF COLUMN PARAMETERS b' AND ρ WITH COLUMN PORE DIAMETER AND SOLUTE MOLECULAR WEIGHT

Study	*Column pore diameter (nm)*	*Solute*	*M*	*b'*	*ρ*
Ref. 12	8	300–6000 dalton peptides *	1100	0.20	0.35
Present study	15	Leucine–enkephalin	600	0.20	0.55
		Bradykinin	1100	0.05	0.45
		Angiotensin I	1300	0.15	0.45
		Glucagon	3500	0.15	0.45
		Insulin	6000	0.15	0.45
		Ribonuclease A	12 500	0.10	0.30
		Lysozyme	14 000	0.05	0.20
Ref. 13	30	Ribonuclease A Cytochrome *c* Lysozyme *	12 800	0.20	0.90
		Carbonic anhydrase	30 000	0.10	0.40
		Transferrin	80 000	0.00	0.30

* Average of three or more compounds.

factor (1.1) in eqn. 6) that have been invoked, it might be questioned whether our model is more than an elaborate exercise in empirical data-fitting. We believe that this is not the case for the following reasons. First, all these effects involving the latter parameters have been confirmed for separations involving small molecules (refs. 26, 32 and present paper). These small-molecule separations are free from many of the complexities of large-molecule separations, and the role of most of these parameters (all but J) is well understood in terms of classical chromatographic theory[32]. Second, values of all but b' and ρ are fixed within narrow limits (or determined by other variables such as $\bar{k}$); only these two parameters were used to fit the present data set [103 values of σ_v, for three different HPLC systems (different laboratories), and with gradient conditions varied over wide limits]. Third, the derived values of b' and ρ correlate roughly with solute molecular weight and column-packing pore size as expected.

On the other hand, we do not claim that the chromatography of these large-biomolecule gradient separations is fully understood. Our model is a first attempt to define the major factors that control these separations. Application of this model to a wider range of reversed-phase systems should further clarify both its strengths and its limitations.

CONCLUSIONS

Experimental band-width data were obtained for the reversed-phase gradient elution separation of seven peptides ranging in molecular weight from 600 to 14 000

daltons. Experimental conditions (gradient range and time, flow-rate) were varied over a wide range, yielding peak-volumes (1 S.D.) of 44–480 μl. A previously proposed model for predicting band-widths in gradient elution was modified in the light of these data; specifically, an anomalous broadening of gradient bands when the gradient is steep and/or the solute is a large molecule (*i.e.* has a large *S*-value) is now taken into account. Application of the model to these experimental data resulted in acceptable agreement between predicted and experimental band-width values ($\pm$ 10–20%, 1 S.D.). Similar agreement was found between experimental and calculated values for two other studies from the literature (peptides/proteins with molecular weights of up to 80 000 daltons).

The present model therefore gives a good account of these separations when the solutes are "well behaved", *i.e.* when secondary retention effects, slow equilibration between native and denatured protein, and other phenomena peculiar to large biomolecules can be effectively ignored. This will often *not* be the case for the separation of proteins by reversed-phase systems. However in these cases it will be apparent that the system is not "well behaved", because experimental band widths will be much larger than values predicted by the model. Then attention can be given to modifying the "chemistry" of the system so as to minimize the importance of these effects.

The present model is also useful in guiding the optimization of peptide/protein separations using reversed-phase gradient elution. Following an initial run, the model (in the form of a computer program) can be used to predict how separation will change with experimental conditions. Examples of this are given in the following paper[33].

Finally, it appears that the separation of these large biomolecules by reversed-phase HPLC proceeds in essentially the same manner as for the isocratic separation of small molecules. This means that the column plate number N plays the same role in controlling sample resolution as in small-molecule chromatography. Apparent exceptions appear to involve either effects arising from "non-well-behaved" systems, or a failure to appreciate how separation conditions affect all gradient elution runs.

SYMBOLS

A, B, C	Coefficients of Knox equation (eqn. 5).
b	Gradient steepness parameter (eqn. 13).
b'	Surface diffusion parameter, equal to solute diffusion coefficient in stationary phase divided by diffusion coefficient in bulk mobile phase.
d_c	Column inside diameter (cm).
D_m	Solute diffusion coefficient in bulk mobile phase (cm^2/sec) (eqn. 4).
d_p	Diameter of column-packing particles (cm).
F	Mobile phase flow-rate (ml/sec).
G	Band compression factor in gradient elution (eqn. 1 of following paper).
h	Reduced plate height (H/d_p).
H	Column plate height (L/N) (cm).
J	Factor by which bands in gradient elution are broadened anomalously (eqns. 11a and 12).
k'	Solute capacity factor.

$\bar{k}$	Mean or effective value of k' in gradient elution; equal to k' for band when it reaches column midpoint.
k_f	k'-value at elution for band in gradient elution (eqn. 8 of following paper).
L	Column length (cm).
N	Column plate number.
M	Solute molecular weight.
PC	Peak capacity of a gradient separation.
S	$-\mathrm{d}(\log k')/\mathrm{d}\varphi$ for a given solute; obtained from relationship $\log k' = \log k_0 - S\varphi$.
T	Temperature of column (°K).
t_G	Gradient time (sec).
u	Mobile phase velocity (cm/sec) (eqn. 1).
V_m	Column dead volume (ml) (eqn. 2).
V_G	Gradient volume, equal $t_G F$ (ml).
x	Fraction of mobile phase inside column that is outside of particle pores.
$\Delta\varphi$	Change in volume-fraction φ of organic solvent in mobile phase during gradient.
φ	Volume fraction of organic solvent in mobile phase.
ν	Mobile phase reduced velocity (eqn. 3).
ρ	Factor by which solute diffusion in particle pores is reduced due to combination of large solute molecule and small pore diameter.
σ_{ec}	Band broadening due to extra-column effects (1 S.D.) (ml) (eqn. 15).
σ_{calc}	Value of σ_v calculated from eqn. 11.
σ_{expt}	Experimental value of σ_v (ml).
σ_t	Band width in gradient elution (1 S.D.) (sec) (eqn. 14).
σ_v	Band volume in gradient elution (1 S.D.) (eqn. 11a) (ml).
σ'_v	Theoretical band volume (1 S.D.) calculated from eqn. 11, assuming $J = 1$ (no anomalous band broadening).
σ_{vT}	Band volume including extra-column contributions (eqn. 11 of following paper).
τ	Detector time constant (sec) (eqn. 15).

REFERENCES

1 M. T. W. Hearn, F. E. Regnier and C. T. Wehr, *Amer. Lab.*, 14 (1982) 18.
2 W. S. Hancock and J. T. Sparrow, in Cs. Horváth (Editor), *High-Performance Liquid Chromatography, Advances and Perspectives, Vol. 3*, Academic Press, New York, 1983, p. 49.
3 M. T. W. Hearn, in Cs. Horváth (Editor), *High-Performance Liquid Chromatography, Advances and Perspectives, Vol. 3*, Academic Press, New York, 1983, p. 87.
4 J. M. Di Bussolo, *Amer. Biotechnology Lab.*, June (1984) 20.
5 J. A. Smith and M. J. O'Hare, *J. Chromatogr.*, 299 (1984) 13.
6 L. A. Witting, D. J. Gisch, R. Ludwig and R. Eksteen, *J. Chromatogr.*, 296 (1984) 97.
7 K. A. Cohen, J. Chazaud and G. Calley, *J. Chromatogr.*, 282 (1983) 423.
8 J. D. Pearson, N. T. Lin and F. E. Regnier, *Anal. Biochem.*, 124 (1982) 217.
9 M. J. O'Hare, M. W. Capp, E. C. Nice, N. H. C. Cooke and B. G. Archer, *Anal. Biochem.*, 126 (1982) 17.
10 N. H. C. Cooke, B. G. Archer, M. J. O'Hare, E. C. Nice and M. Capp, *J. Chromatogr.*, 255 (1983) 115.
11 F. E. Regnier and R. Noel, *J. Chromatogr. Sci.*, 14 (1976) 32.
12 J. L. Meek and Z. L. Rossetti, *J. Chromatogr.*, 211 (1981) 15.

13 E. C. Nice, M. W. Capp, N. Cooke and M. J. O'Hare, *J. Chromatogr.*, 218 (1981) 569.
14 R. V. Lewis, A. Fallon, S. Stein, K. D. Gibson and S. Udenfriend, *Anal. Biochem.*, 104 (1980) 153.
15 E. C. Nice, M. Capp and M. J. O'Hare, *J. Chromatogr.*, 185 (1979) 413.
16 J. D. Pearson, W. C. Mahoney, M. A. Hermodson and F. E. Regnier, *J. Chromatogr.*, 207 (1981) 325.
17 K. J. Wilson, E. van Wieringen, S. Klauser, M. W. Berchtold and G. J. Hughes, *J. Chromatogr.*, 237 (1982) 407.
18 J. D. Pearson and F. E. Regnier, *J. Liq. Chromatogr.*, 6 (1983) 497.
19 R. V. Lewis and D. De Wald, *J. Liq. Chromatogr.*, 5 (1982) 1367.
20 M. T. W. Hearn and B. Grego, *J. Chromatogr.*, 296 (1984) 61.
21 G. Lindgren, B. Lundström, I. Källman and K.-A. Hansson, *J. Chromatogr.*, 296 (1984) 83.
22 D. W. Armstrong and R. E. Boehm, *J. Chromatogr. Sci.*, 22 (1984) 378.
23 L. R. Snyder, M. A. Stadalius and M. A. Quarry, *Anal. Chem.*, 55 (1983) 1412A.
24 R. R. Walters, *J. Chromatogr.*, 249 (1982) 19.
25 C. N. Satterfield, C. K. Colton and W. H. Pitcher, *Am. Inst. Chem. Eng. J.*, 19 (1973) 62826.
26 L. R. Snyder, in Cs. Horváth (Editor), *High-Performance Liquid Chromatography, Advances and Perspectives, Vol. 1*, Academic Press, New York, 1980, p. 207.
27 M. A. Stadalius, *Ph.D. Thesis*, University of Delaware, June 1984.
28 S. A. Cohen, S. Dong, K. P. Benedek and B. L. Karger, in I. Chaiken, M. Wilchek and I. Pasikh (Editors), *Symposium Proceedings, 5th International Symposium on Affinity Chromatography and Biological Recognition*, Academic Press, New York, 1984, p. 479.
29 S. A. Cohen, K. P. Benedek, S. Dong, Y. Tapui and B. L. Karger, *Anal. Chem.*, 56 (1984) 217.
30 K. A. Cohen, K. Schnellenberg, K. Benedek, B. L. Karger, B. Grego and M. T. W. Hearn, *Anal. Biochem.*, 140 (1984) 223.
31 M. A. Stadalius, H. S. Gold and L. R. Snyder, *J. Chromatogr.*, 296 (1984) 31.
32 R. W. St' ut, J. J. DeStefano and L. R. Snyder, *J. Chromatogr.*, 282 (1983) 263.
33 M. A. Stadalius, M. A. Quarry and L. R. Snyder, *J. Chromatogr.*, 327 (1985) 93–113.
34 A. J. Banes, G. W. Link and L. R. Snyder, *J. Chromatogr.*, 326 (1985) 419.
35 M. A. Quarry, R. L. Grob and L. R. Snyder, *J. Chromatogr.*, 285 (1983) 1, 19.
36 M. A. Quarry, R. L. Grob and L. R. Snyder, *Anal. Chem.*, submitted for publication.
37 M. E. Young, P. A. Carroad and R. L. Bell, *Biotechnol. Bioeng.*, 22 (1980) 947–955.
38 R. R. Walters, J. F. Graham, R. M. Moore and D. J. Anderson, *Anal. Biochem.*, 140 (1984) 190–195.
39 L. R. Snyder and J. J. Kirkland, *Introduction to Modern Liquid Chromatography*, 2nd ed., Wiley-Interscience, New York, 1979.
40 X. Geng and F. E. Regnier, *J. Chromatogr.*, 296 (1984) 15.
41 H. Poppe, unpublished results.
42 R. W. Stout, J. J. DeStefano and L. R. Snyder, *J. Chromatogr.*, 261 (1983) 189.
43 J. P. Larmann, J. J. DeStefano, A. P. Goldberg, R. W. Stout, L. R. Snyder and M. A. Stadalius, *J. Chromatogr.*, 225 (1983) 163.
44 J. W. Dolan, J. R. Gant and L. R. Snyder, *J. Chromatogr.*, 165 (1979) 31.
45 H. Elgass, *Ph.D. Dissertation*, Universität des Saarlandes, Saarbrücken, 1978, p. 59.
46 L. R. Snyder and P. E. Antle, *LC, Liq. Chromatogr. HPLC Mag.*, 3 (1985) 98.